International Journal of Mass Spectrometry 302 (2011) 157–166

Contents lists available at ScienceDirect

International Journal of Mass Spectrometry

journal homepage: www.elsevier.com/locate/ijms

Cooperativity and allostery in cAMP-dependent activation of Protein Kinase A: Monitoring conformations of intermediates by amide hydrogen/deuterium exchange☆

Balakrishnan Shenbaga Moorthy[1], Suguna Badireddy[1], Ganesh S. Anand*

Department of Biological Sciences, National University of Singapore 14 Science Dr 4, Singapore 117543, Singapore

ARTICLE INFO

Article history:
Received 7 June 2010
Received in revised form 26 August 2010
Accepted 9 September 2010
Available online 17 September 2010

Keywords:
Allostery
Intermediate
cAMP
Cooperativity
Conformational change
Dynamic

ABSTRACT

Amide hydrogen/deuterium exchange mass spectrometry is a powerful method both for mapping protein–protein interactions and measuring conformational dynamics of protein complexes. In this study we report its application to monitoring the stepwise process governing cAMP-dependent activation of Protein Kinase A (PKA). In the absence of cAMP, PKA exists in an inactive complex of catalytic (C) and regulatory (R) subunits. cAMP binding induces large conformational changes within the R-subunit leading to dissociation of the active C-subunit. Although crystal structures of end-point, inactive and active states are available, the molecular basis for cooperativity in cAMP-dependent activation of PKA is not clear. In this study we report application of amide hydrogen/deuterium exchange mass spectrometry on tracking the stepwise cAMP-induced conformational changes using a single point mutant (R209K) at the cyclic nucleotide binding domain (CNB)-A site. Our amide exchange results reveal that binding of one molecule of cAMP increases amide exchange in important regions within the second CNB-B domain. Increased exchange was also seen at the interface between CNB-B and the C-subunit suggesting weakening of the R–C interface without dissociation. Importantly, binding of the first molecule of cAMP greatly increases the conformational mobility/dynamics of two key regions coupling the two CNBs, the αC/C′:A and αA:B helix. We believe that the enhanced dynamics of these regions forms the basis for the positive cooperativity in the cAMP-dependent activation of PKA. In summary, our results reveal the close allosteric coupling between CNB-A and CNB-B with the C-subunit providing important molecular insights into the function of CNB-B domain.

1. Introduction

Cyclic 3′5′ adenosine monophosphate (cAMP) is an important second messenger that enables cells to sense and respond to hormonal stimuli. The *c*yclic *n*ucleotide *b*inding (CNB) domain is an ancient motif that appears to have co-evolved as the primary receptor for cAMP [1]. CNBs function as regulatory modules in different classes of proteins and in eukaryotes, one of the principal targets of cAMP is the cAMP-dependent protein kinase, Protein Kinase A (PKA), whose regulatory subunit (R-subunit) contains two tandem CNBs. In the absence of cAMP, PKA exists as an inactive tetrameric holoenzyme with the homodimeric R-subunits bound to two catalytic (C) subunits. cAMP binding to the CNBs of the R-subunits induces conformational changes, leading to dissociation of the C-subunit and activation of PKA [2]. Out of 4 isoforms of the C and R subunits, Cα and RIα are most widely distributed throughout all mammalian tissue and are the most important isoforms of PKA [3]. PKA R-subunit is an extended molecule containing an N-terminal dimerization domain and a pseudosubstrate region followed by CNB-A and CNB-B respectively (Fig. 1A). The R-subunit lacking the N-terminal dimerization domain, RIα(92–379), retains high-affinity binding to the C-subunit and provides a minimal monomeric model for examining R–C interactions as well as cAMP binding to CNB-A and CNB-B (Fig. 1A) [4,5]. A specific conserved set of residues critical for binding to cAMP is referred to as the phosphate binding cassette (PBC) (PBC:A and PBC:B for CNB-A and CNB-B respectively) [1]. In contrast, PKA C-subunit is a globular

Abbreviations: BME, β-mercaptoethanol; cAMP, cyclic 3′5′adenosine monophosphate, C, catalytic subunit of cAMP-dependent protein kinase; R, regulatory subunit of cAMP-dependent protein kinase; PKA, cAMP-dependent protein kinase, Protein Kinase A; RIα(92–379), deletion mutant of type Iα isoform of the R-subunit; CNB, cyclic nucleotide binding domain; PBC, phosphate binding cassette; MOPS, 3-(N-Morpholino)-propane-sulfonic acid; TFA, trifluoroacetic acid.

☆ This work was supported by a grant from A*STAR-Biomedical Research Council, Singapore and a Beta-test agreement and grant from Waters Corporation, Milford MA.

* Corresponding author. Tel.: +65 6516 7722; fax: +65 6779 2486.
E-mail address: dbsgsa@nus.edu.sg (G.S. Anand).

[1] BSM and SB contributed equally to this work.

1387-3806/$ – see front matter © 2010 Elsevier B.V. All rights reserved.
doi:10.1016/j.ijms.2010.09.012

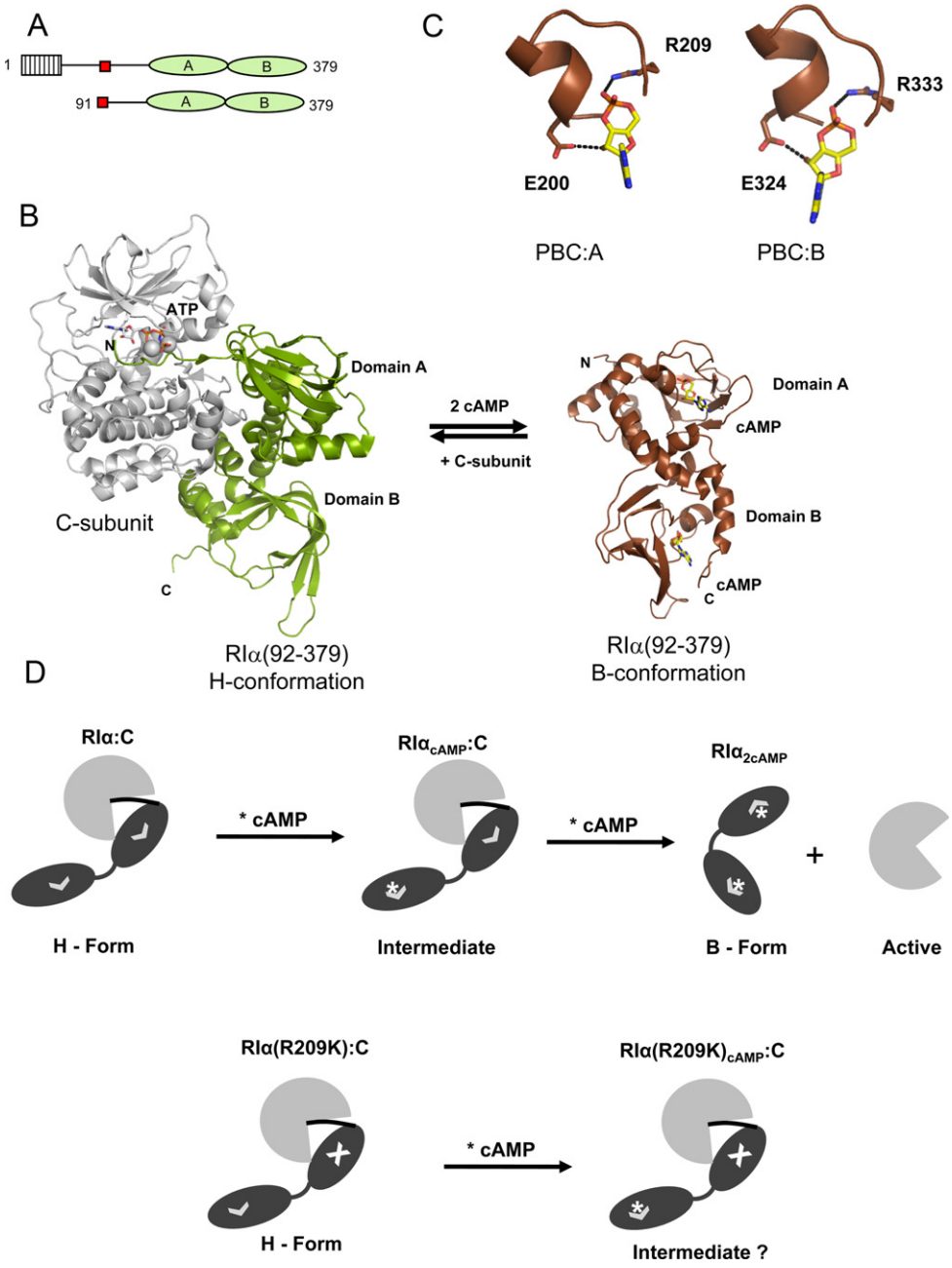

Fig. 1. A: Domain organization of RIα showing an N-terminal dimerization/docking domain (D/D) (gray hashed box) connected by a linker to two tandem cAMP-binding domains, CNB-A and CNB-B in green. The linker contains a PKA pseudosubstrate site which is essential for facilitating interactions of RIα with the C-subunit in red. B: Mechanism of type I PKA regulation. In PKA holoenzyme, the C-subunit (gray) is kept inactivated by the R-subunit (green) (structure of the RIα(92–379):C holoenzyme complex (PDB ID: 2QCS). Note the structure of the RIα(92–379):C holoenzyme complex solved by X-ray crystallography was of a point mutant, RIα (92–379)R333K in complex with the C-subunit [4]. ATP and the pseudosubstrate region occupy the active site cleft formed by the two lobes of the C-subunit. Binding of 2 molecules of cAMP to CNB-A and CNB-B of the holoenzyme induces conformational changes leading to dissociation of the C-subunit and its activation. The R-subunit thus adopts distinct conformations, bound to C-subunit (green, H-conformation) [4] and bound to cAMP (brown, B-conformation) (PDB ID: 1RGS) [5]. C: Close-up of the Phosphate binding cassettes (PBC) (brown) from both CNB-A and CNB-B. In PBC:A, the critical conserved residues Arg 209 and Glu 200 and in PBC:B, Arg 333 and Glu 324 together with backbone amide nitrogen atoms of residues in the PBC anchor the cyclic phosphate and 2′OH moieties of cAMP (yellow) respectively. D: Cartoon showing stepwise cAMP-mediated activation of PKA (* represents a molecule of cAMP, X represents a point mutation that abolishes high-affinity binding of cAMP). Activation of type I PKA is cooperative and sequential with cAMP binding first to CNB-B and then to CNB-A. Mutation of Arg 209 to a Lys in CNB-A of R-subunit abolishes high-affinity cAMP binding to the CNB-A without significantly affecting binding of cAMP to CNB-B. The holoenzyme, RIα(92–379)R209K:C provides an ideal model system to probe the effects of a single molecule of cAMP binding to CNB-B and to study effects of a single cAMP-bound intermediate in the cAMP-dependent activation pathway of PKA. (For interpretation of the references to color in this figure legend, the reader is referred to the web version of the article.)

protein with a bilobal structure characteristic of all kinases, where the small N-terminal lobe and larger C-terminal lobe enclose a cleft which binds ATP and provides binding sites for substrates or inhibitors [6].

Structures of cAMP-bound conformations of the CNB domain, denoted the 'B-conformation', reveal a highly conserved architecture with two subdomains: a β-subdomain with an eight-stranded β-sheet, containing the solvent-shielded pocket for binding cAMP and a non-contiguous α-subdomain. The structure of a PKA holoenzyme complex [4,7] revealed a large conformational change in the R-subunit which is denoted as the 'H-conformation' (Fig. 1B). The PBC region within the β-subdomain reveals a conserved

Table 1
Effect of cAMP binding on the R-subunit (peptides from RIα(92–379)R209K:C holoenzyme and RIα(92–379)R209K) measured by amide H/D exchange.

R-subunit pepsin digest fragments (sequence) (*m*/*z*)	Charge (*z*)	Maximum exchangeable amides	Maximum deuterons exchanged after 10 min		
			RIα(92–379) R209K:C	RIα(92–379) R209K:C + cAMP	RIα(92–379) R209K + cAMP
EVYTEE (101–106) (769.33)	1	5	3.0 ± 0.06	3.3 ± 0.00	4.0 ± 0.05
YVRKVIPKDYKTMAA (111–125) (446.50)	4	13	10.5 ± 0.21	10.7 ± 0.10	12.1 ± 0.05
YVRKVIPKDYKTMAALAKAIEKNVL (111–135) (573.34)	5	23	14.6 ± 0.28	15.9 ± 0.60	17.0 ± 0.07
FSHLDDNERSDIF (136–149) (797.86)	2	12	1.7 ± 0.02	1.7 ± 0.01	3.7 ± 0.04
IAGETVIQQGDEGDNF (157–172) (846.89)	2	15	6.7 ± 0.08	6.4 ± 0.10	6.7 ± 0.19
YVIDQGEMDV (173–182) (1168.52)	1	9	1.3 ± 0.01	1.3 ± 0.00	1.8 ± 0.03
DVYVNNE (181–187) (852.37)	1	6	3.1 ± 0.07	3.0 ± 0.10	2.6 ± 0.01
WATSVGEGGSF (188–198) (1097.49)	1	10	5.0 ± 0.00	5.5 ± 0.10	6.8 ± 0.12
FGELALI (198–204) (762.44)	1	6	2.5 ± 0.05	1.2 ± 0.10	0.1 ± 0.02
ALIYGTPKAAT (202–212) (553.32)	2	9	5.7 ± 0.07	6.3 ± 0.00	7.9 ± 0.08
ALIYGTPKAATVKAKT (202–217) (545.00)	3	14	6.1 ± 0.01	7.6 ± 0.30	9.1 ± 0.47
VKAKTNVKL (213–221) (500.83)	2	8	1.7 ± 0.04	1.5 ± 0.10	1.8 ± 0.03
WGIDRDSY (222–229) (506.23)	2	6	0.9 ± 0.00	0.8 ± 0.00	1.3 ± 0.02
RRILMGSTL (230–238) (523.81)	2	8	1.3 ± 0.00	2.4 ± 0.00	3.4 ± 0.03
RKRKMYEEF (239–247) (643.84)	2	8	2.2 ± 0.02	4.1 ± 0.00	4.6 ± 0.05
LSKVSIL (248–254) (759.50)	1	6	2.5 ± 0.02	3.1 ± 0.10	3.1 ± 0.02
LSKVSILESLDKWERLTVADALE (248–270) (872.48)	3	22	8.6 ± 0.18	16.1 ± 0.50	10.0 ± 0.06
TVADALEPVQ (264–273) (521.77)	2	8	3.1 ± 0.02	3.6 ± 0.00	3.4 ± 0.01
PVQFEDGQKIVVQGEPGDE (271–289) (1036.00)	2	16	6.3 ± 0.09	5.3 ± 0.10	5.4 ± 0.09
EDGQKIVVQGEPGDEF (275–290) (873.91)	2	14	4.2 ± 0.03	3.0 ± 0.20	3.0 ± 0.05
IILEGSAAVL (292–301) (493.30)	2	9	3.7 ± 0.13	3.7 ± 0.10	4.5 ± 0.01
QRRSENEEF (302–310) (597.78)	2	8	4.0 ± 0.02	4.0 ± 0.00	4.6 ± 0.06
VEVGRLGPSDYFGE (311–324) (762.87)	2	12	3.7 ± 0.06	3.1 ± 0.00	1.8 ± 0.03
FGEIAL (322–327) (649.36)	1	5	2.1 ± 0.03	1.1 ± 0.10	0.2 ± 0.11
LMNRPRAAT (328–336) (515.28)	2	7	3.9 ± 0.02	2.9 ± 0.10	1.6 ± 0.05
VARGPLKC (338–345) (422.25)	2	5	0.7 ± 0.02	0.6 ± 0.00	0.4 ± 0.13
VKLDRPRF (346–353) (515.81)	2	6	0.7 ± 0.00	1.0 ± 0.10	1.3 ± 0.03
ERVLGPCSD (354–362) (975.45)	1	7	2.3 ± 0.03	3.1 ± 0.00	3.2 ± 0.04
ILKRNIQQYNSF (363–374) (762.42)	2	11	9.0 ± 0.09	8.5 ± 0.00	6.8 ± 0.03

Values reported are the mean and standard error calculated from two independent experiments. All deuterium exchange values reported were corrected for ~33% back exchange by multiplying the raw centroid values by a factor of 1.49.

Table 2
Effect of cAMP binding on the C-subunit (peptides from RIα(92–379)R209K:C holoenzyme) measured by amide H/D exchange.

C-subunit pepsin digest fragments (Sequence) (*m*/*z*)	Charge (*z*)	Maximum exchangeable amides	Maximum deuterons exchanged after 10 min	
			RIα(92–379) R209K:C	RIα(92–379) R209K:C + cAMP
FLAKAKED (18–25) (461.25)	2	7	4.5 ± 0.48	4.7 ± 0.04
LKKWETPSQNTAQL (27–40) (822.44)	2	12	8.1 ± 0.07	7.8 ± 0.06
TPSQNTAQLDQFDRIKTLGTG–SFGRVMLVKHKESGNHYAMK (32–72) (919.08)	5	39	12.7 ± 0.14	13.2 ± 0.10
IEHTLNE (85–91) (428.22)	2	6	0.2 ± 0.04	0.4 ± 0.01
KRILQAVNFPFL (92–103) (723.44)	2	10	2.2 ± 0.00	2.0 ± 0.00
VKLEFSFKDNSNL (104–116) (770.91)	2	12	2.5 ± 0.01	2.2 ± 0.05
VMEYVAGGEMFSH (119–131) (728.84)	2	12	0.3 ± 0.02	0.4 ± 0.09
EMFSHLRRIGR (127–137) (701.38)	2	10	6.4 ± 0.29	6.3 ± 0.21
RRIGRFSEPHARF (133–145) (427.97)	4	11	1.4 ± 0.00	1.3 ± 0.02
IVLTF (150–154) (592.37)	1	4	0.1 ± 0.05	0.1 ± 0.06
FEYLHSLDLI (154–163) (625.33)	2	9	0.2 ± 0.01	0.3 ± 0.01
IYRDLKPENLL (163–173) (687.40)	2	9	0.5 ± 0.00	0.6 ± 0.01
LIDQQG (173–178) (673.35)	1	5	1.5 ± 0.02	1.4 ± 0.02
YIQVTDFGF (179–187) (942.46)	1	8	0.3 ± 0.00	0.3 ± 0.00
AKRVKGRTWTLCGTPEYLAPEIIL (188–211) (932.50)	3	21	3.0 ± 0.05	3.5 ± 0.02
SKGYNKAVDWWALGVL (212–227) (903.98)	2	15	1.9 ± 0.01	1.9 ± 0.04
IYEMAAGYPPFFADQPIQ (228–245) (1029.49)	2	14	6.1 ± 0.08	6.2 ± 0.09
YEKIVSGKVRFPSHFSSDLKDLLRNLL (247–273) (633.16)	5	25	4.5 ± 0.02	4.5 ± 0.00
QVDLTKRFGNLKNGVNDIKNHKW (274–296) (681.88)	4	22	7.5 ± 0.07	8.5 ± 0.20
FATTDW (297–302) (740.33)	1	5	3.4 ± 0.05	2.9 ± 0.02
IAIYQRKVEAPFIPKFKGPGDTSN (303–326) (669.87)	4	20	10.0 ± 0.16	9.5 ± 0.03
FDDYEE (327–332) (817.29)	1	4	2.6 ± 0.01	2.5 ± 0.05
DDYEEE (328–333) (799.27)	1	5	3.4 ± 0.09	3.0 ± 0.02
IRVSINEKCGKE (335–346) (485.91)	3	11	7.1 ± 0.13	6.9 ± 0.02

Values reported are the mean and standard error calculated from two independent experiments. All deuterium exchange values reported were corrected for ~33% back exchange by multiplying the raw centroid values by a factor of 1.49.

hydrogen bonding network, connecting residues that are critical for specific binding to cAMP [1]. The key residues include single conserved arginines in both domains, Arg 209 and Arg 333, which are important for anchoring the phosphate moiety of cAMP (Fig. 1C). cAMP binding to CNB-A and anchoring of the cyclic AMP phosphate with Arg 209 is critical for the activation of C-subunit as it has been shown that the R209K mutation abolishes the tight binding of cAMP at CNB-A [8] and blocks activation of PKA.

It has been known that cAMP binds the PKA holoenzyme in a positive cooperative manner wherein a first molecule of cAMP binds first to the CNB-B domain followed by binding to CNB-A, leading to holoenzyme dissociation and activation [8,9]. Although numerous crystal structures of free individual R-subunits and in complex with the C-subunit have been solved, providing high-resolution insights into the end-point conformations of PKA, the molecular basis for cooperativity and allosteric coupling of the two cAMP binding events is not clear as it requires structural characterization of an intermediate state with the CNB-B domain alone bound to a single molecule of cAMP (Fig. 1D). NMR studies on the wild-type and single point mutants of RIα(119–379) have revealed the connectivity between CNB-A and CNB-B domains [10] but they still do not describe the conformation of an intermediate in the cAMP-mediated activation pathway, namely of the holoenzyme state bound to a single cAMP molecule at CNB-B. Amide hydrogen/deuterium exchange coupled with ESI-QTOF mass spectrometry is a powerful tool to study protein–protein interactions and monitor conformational dynamics of proteins [11]. We have used this technique to characterize an important intermediate in the cAMP activation pathway of PKA by monitoring the effects of cAMP binding to the point mutant RIα(92–379) R209K. The X-ray crystal structure of holoenzyme (PDB ID: 2QCS) has revealed four sites on the R-subunit that interact with the C-subunit in the holoenzyme complex [4], one site contributed by the pseudosubstrate site, two contributed by CNB-A and one by CNB-B. Our amide exchange results reveal that binding of one molecule of cAMP increases deuterium exchange in two key regions, the αC/C′ of CNB-A domain (αC/C′:A) and αA helices of the CNB-B domain (αA:B). The αC/C′ of CNB-A domain undergoes the largest conformational rearrangements between the cAMP-bound and C-subunit-bound conformations of the R-subunit [7], while the αA helix of the CNB-B domain (αA:B) contains W260, a key aromatic capping residue that serves to stabilize binding of a second molecule of cAMP to CNB-A [1]. We believe the increased exchange in these regions reflects enhanced conformational mobility/dynamics which facilitates binding of a second molecule of cAMP to CNB-A providing the basis for the positive cooperativity in the cAMP-dependent activation of PKA.

2. Materials and methods

2.1. Reagents

BL21 (DE3) *E. coli* strains were from Novagen (Madison, WI). TALON metal affinity resin was from Clontech Laboratories (Mountain View, CA). 8-AminoEthylAmino (AEA)-cAMP was from Biolog Life Science Institute (Bremen, Germany). ATP and cAMP were obtained from Sigma–Aldrich Corp. (Singapore). Poroszyme immobilized pepsin cartridge was from Applied Biosystems (Foster City, CA). Deuterium oxide (99.9% deuterium) was obtained from Sigma-Aldrich Corp. (Singapore). Trifluoroacetic acid (TFA) and acetonitrile were from Fisher Scientific (Singapore). All other chemicals were at least reagent grade.

2.2. Purification of RIα(92–379)(R209K) and C-subunit

cAMP affinity chromatography resin for R-subunit purification was synthesized by coupling 8-AEA-cAMP to the NHS-activated sepharose 4 Fast Flow® beads as recommended (GE Life Sciences, Singapore). cAMP-free RIα(92–379)R209K was expressed and purified as described previously [8,12]. Hexahistidine tagged C-subunit of PKA was expressed and purified as described previously [13]. The holoenzyme, RIα(92–379)R209K:C was purified by size exclusion-gel filtration chromatography on an AKTA system (GE Life Sciences) as described earlier [8] by using the buffer 50 mM MOPS, pH 7.0, 50 mM NaCl, 2 mM $MgCl_2$, 0.2 mM ATP and 5 mM BME.

2.3. Amide hydrogen/deuterium exchange mass spectrometry

The size exclusion chromatography purified cAMP-free RIα(92–379)R209K:C holoenzyme complex was concentrated to 50 μM using vivaspin concentrators (Sartorius Stedim Biotech GmbH, Goettingen, Germany). 2 μL of the samples in storage buffer (20 mM Tris–HCl, pH 7.5, 50 mM NaCl, 10 mM $MgCl_2$, 5 mM BME) were diluted and incubated with 18 μL of D_2O (99.90%) resulting in a final deuterium concentration of 90% in buffer A (20 mM MOPS, pH_{read} 7.0, 50 mM NaCl, 2 mM $MgCl_2$, 0.2 mM ATP, 5 mM BME). Amide exchange was carried out at 20 °C for various time points (0.5, 1, 2, 5 and 10 min). In order to test the effects of cAMP binding to CNB-B of RIα of the holoenzyme, we incubated the 50 μM R:C holoenzyme complex with a final concentration of 70 μM cAMP. Given a Kd of the CNB-B domain in the holoenzyme complex for cAMP (Kd ~ 0.8 μM for CNB-B domain) [8], we predicted that the CNB-B domain site of the protein complex would be completely saturated with cAMP allowing for characterization of a single cAMP-bound holoenzyme intermediate. Deuterium exchange reactions were carried out for both holoenzyme samples in the presence and absence of cAMP and cAMP-bound RIα(92–379)R209K as described previously [24]. The exchange reaction was quenched by addition of 40 μL of pre-chilled 0.1% TFA to get a final pH_{read} of 2.5. 50 μL of the quenched sample (~100 pmol protein sample) was then injected on to a chilled nano-UPLC sample manager (beta test version, Waters, Milford, MA) as previously described [14]. The sample was run through a 2.1 × 30 mm immobilized pepsin column (Porozyme, ABI, Foster City, CA) using 100 μL/min 0.05% formic acid in water. The digested peptides were trapped on a 2.1 × 5 mm C18 trap (ACQUITY BEH C18 VanGuard Pre-column, 1.7 μm, Waters, Milford, MA) and eluted using an 8–40% gradient of acetonitrile in 0.1% formic acid at 40 μL/min, supplied by a nanoACQUITY Binary Solvent Manager (Waters, Milford, MA), on to a reverse phase column (ACQUITY UPLC BEH C18 Column, 1.0 × 100 mm, 1.7 μm, Waters, Milford, MA) for resolution. Peptides were detected and mass measured on a SYNAPT HDMS mass spectrometer (Waters, Manchester, UK) acquiring in MS^E mode [15,16].

Peptides were identified from MS^E data in the non-deuterated samples using ProteinLynx Global Server 2.4 (beta test version) (Waters, Milford, MA) [17,18]. Identifications were only considered if they appeared at least twice out of three replicate runs. These identifications were mapped on to subsequent deuteration experiments using prototype custom software (HDX browser, Waters, Milford, MA). Data on each individual peptide at all time points were extracted using this software, and exported to HX-Express [19] for analysis.

Continuous instrument calibration was carried out with Glu-Fibrinogen peptide (GFP) at 100 fmol/μL. We also visually analyzed the data to ensure only well-resolved peptide isotopic envelopes were subjected to quantitative analysis. A control experiment was

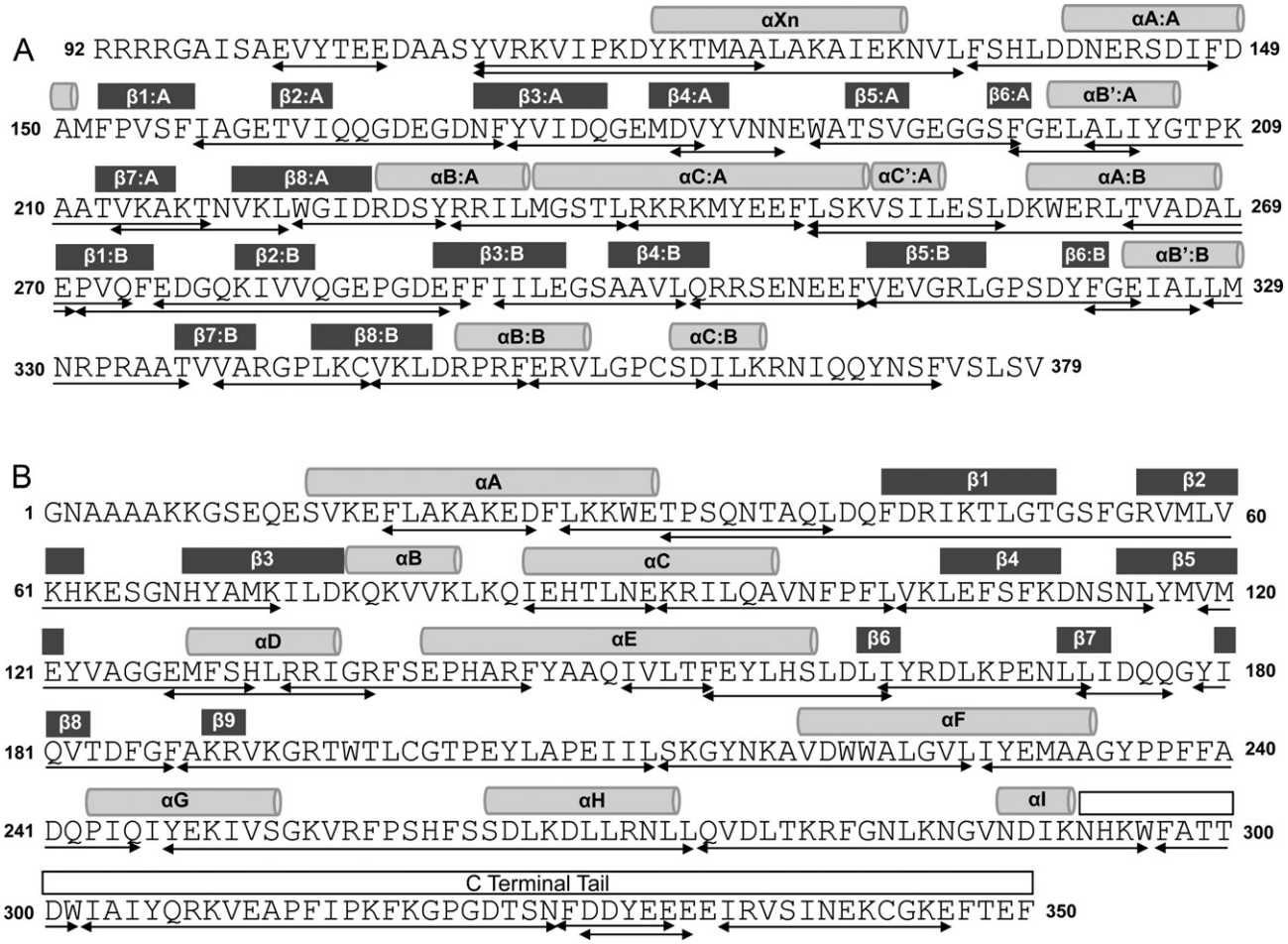

Fig. 2. Sequence coverage map for the R and C-subunit. Amino acid sequence of (A) RIα(92–379)R209K and (B) C-subunit showing secondary structure elements with boundaries. Solid lines denote the pepsin digest fragments analyzed in the study with a total sequence coverage of 90% and 88% for RIα and C-subunit respectively.

carried out to calculate the deuterium back exchange loss during the experiment as described previously [24]. Briefly, this was carried out by incubating ligand-free RIα(91–244) with deuterated buffer A for 24 h at room temperature (20 °C). Even after extended deuteration, RIα(91–244) still showed some ordered regions that were not completely deuterated. For an accurate measurement of back exchange loss, we therefore focused only on peptides from within highly solvent exchangeable regions of the protein, identified as those regions that show greater relative exchange at shorter time points (10 min exchange). The region in RIα(91–244) spanning residues 111–130 is a highly solvent exchangeable region and all 3 overlapping peptides used for calculations of back exchange span this region and showed nearly maximal exchange in ligand-free RIα(91–244) following 10 min deuterium exchange and would thus represent fully deuterated samples following 24 h exchange. An average deuteration back exchange of ~33% was calculated from average back exchange values for 3 peptides: RIα(111–123) (m/z = 547.65) (back exchange – 34.4%), RIα(111–126) (m/z = 632.701) (back exchange = 30.4%) and RIα(111–119) (m/z = 595.34) (back exchange = 33.7%). All deuterium exchange values reported were corrected for a 33% back exchange by multiplying the raw centroid values by a multiplication factor of 1.49 [24]. The analyzed data were then mapped on to the crystal structures of PKA holoenzyme (PDB ID: 2QCS) [4] and that of cAMP-bound RIα(92–379) (PDB ID: 1RGS) [5]. The data shown in Figs. 3 and 4 and Tables 1 and 2 are from replicate, independent experimental measurements.

3. Results and discussion

To monitor the stepwise cooperative activation of type I PKA by cAMP, we used amide H/D exchange measured by ESI-QTOF mass spectrometry. The RIα(92–379)R209K:C holoenzyme was used as a model to monitor the effects of binding of a single cAMP molecule to the CNB-B domain, thereby enabling probing of the conformation of a key intermediate in the activation pathway. Furthermore, this also enabled us to unravel the role of CNB-B domain in mediating the cooperative activation of PKA. We first set out to measure amide H/D exchange of the RIα(92–379) R209K:C holoenzyme both in the presence and absence of cAMP and cAMP-bound RIα(92–379)R209K. Mutation of Arg 209 to a lysine within the PBC:A of RIα abolishes high-affinity binding of cAMP to CNB-A site, without significantly altering cAMP binding to CNB-B [8]. Binding of a single molecule of cAMP to CNB-B induced both local changes within PBC:B as well as global changes in rest of the R-subunit and regions of the C-subunit involved in mediating specific interface contacts with CNB-B. The results are organized to describe: (i) local effects within PBC-B, (ii) changes observed at regions spanning the R–C interface and (iii) global changes within the R-subunit outside PBC-B.

3.1. Pepsin digestion of RIα(92–379)R209K and C-subunit

A total of 29 pepsin digest fragments for RIα(92–379)R209K and 24 fragments for the C-subunit were detected and analyzed in this study. These covered 90% and 88% of their respective pri-

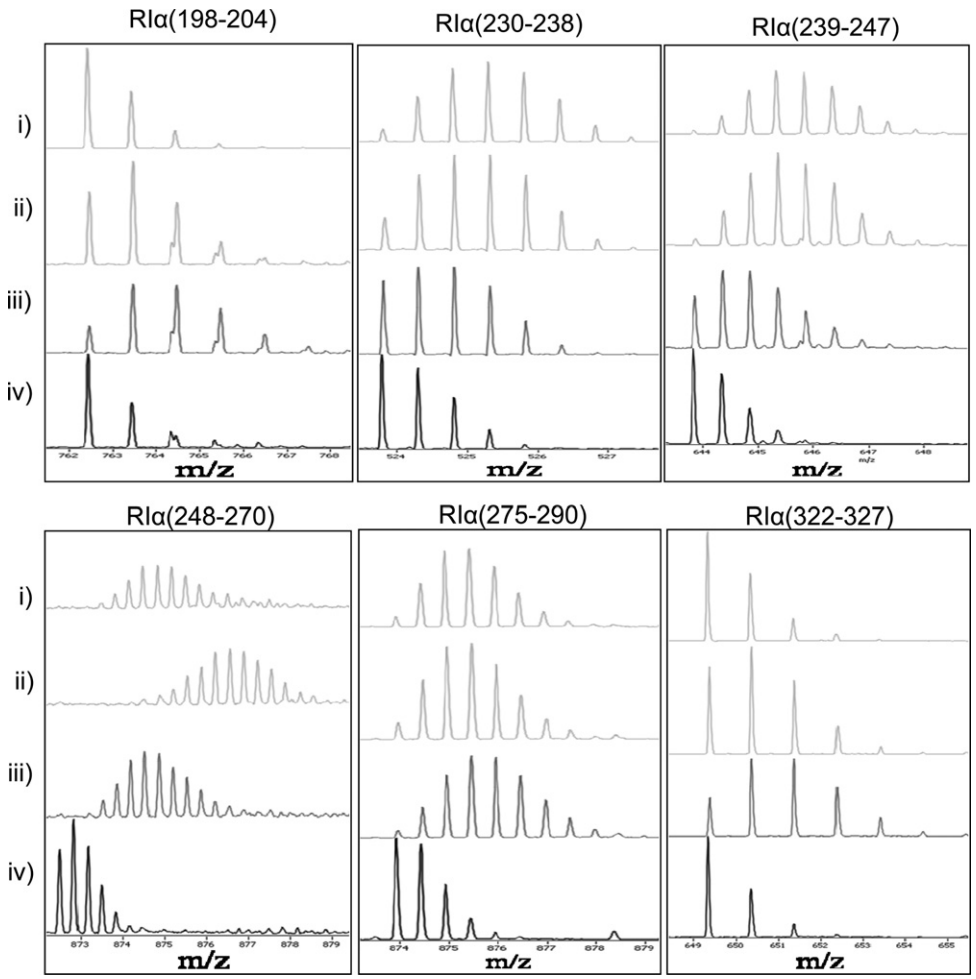

Fig. 3. ESI-QTOF mass spectra of pepsin digest fragments from 6 different regions of RIα(92–379)R209K from the R:C holoenzyme that showed the largest changes in amide H/D exchange upon binding cAMP. The peptides are m/z = 762.44, z = 1, RIα (198–204); m/z = 523.81, z = 2, RIα (230–238); m/z = 643.84, z = 2, RIα (239–247); m/z = 872.48, z = 3, RIα (248–270); m/z = 873.91, z = 2, RIα (275–290); m/z = 649.36, z = 1, RIα (322–327)). i) The isotopic envelope for the peptides from cAMP-bound RIα(92–379)R209K subunit after 10 min deuteration. ii) The isotopic envelope for the peptides from cAMP-bound RIα(92–379)R209K:C holoenzyme after 10 min deuteration. iii) The isotopic envelope for the peptides from cAMP-free RIα(92–379)R209K:C holoenzyme after 10 min deuteration. iv) Undeuterated isotopic envelope of six R-subunit peptides from RIα(92–379)R209K.

mary sequences (Fig. 2A and B). The average numbers of deuterons exchanged (10 min) for each of the peptides were calculated as described in Section 2 and are summarized in Tables 1 and 2. A comparison of average deuteration after ten minutes has provided insights into the effects of cAMP and C-subunit binding in earlier studies [20] and in our study was used to monitor the effects of cAMP binding to the CNB-B domain. For those segments (6 R-subunit peptides) showing the most significant changes observed upon cAMP binding, electrospray ionization time-of-flight (ESI-TOF) spectra are shown in Fig. 3 and plots of the time-course of deuteration are shown in Fig. 4.

3.2. cAMP binding to RIα(92–379)R209K:C holoenzyme does not lead to dissociation of the complex

Binding of cAMP to the RIα(92–379)R209K:C holoenzyme complex under our deuterium exchange reaction conditions did not lead to dissociation of the holoenzyme confirmed by comparing the deuterium exchange of our results with earlier studies on free RIα and holoenzyme complexes [20]. In the holoenzyme, the N-terminal pseudosubstrate regions were completely shielded from solvent in contrast to the free, unbound state [20,21]. We observed the same effects in the N-terminal pseudosubstrate region from our samples of the cAMP-bound RIα(92–379)R209K:C holoenzyme. This is entirely consistent with previous studies that showed cAMP binding to CNB-B in the RIα(92–379)R209K:C holoenzyme failed to dissociate the C and R-subunits [8].

3.3. cAMP binding to RIα(92–379) R209K:C holoenzyme decreases deuterium exchange in PBC:B

The regions from CNB-B of RIα spanning peptides (271–289), (275–290), (311–324), (322–327), (328–336) showed decreased exchange upon binding of cAMP. This is a direct result of binding interactions of these residues with cAMP. From the crystal structure of cAMP-bound RIα(113–379) [5], it can be seen that the residues which form part of CNB-B include Arg 333, Glu 289 and Glu 324 (Fig. 5B). Arg 333 in PBC:B hydrogen bonds directly with the equatorial exocyclic oxygen of the cAMP phosphate and also forms salt bridges with Glu 289. Additionally, the backbone amide nitrogens of residues Gly 323, Ala 326 and Ala 335 also mediate interactions with cAMP. The decreased exchange observed in our experiments thus reflects binding of 1 molecule of cAMP to PBC:B (Figs. 3 and 4 – peptides, RIα(322–327) and RIα(275–290)).

Comparison of the amide exchange in the cAMP-bound RIα(92–379)R209K:C holoenzyme and cAMP-bound RIα(92–379)R209K showed some differences. While the exchange measured was similar in certain regions, the magnitude of amide

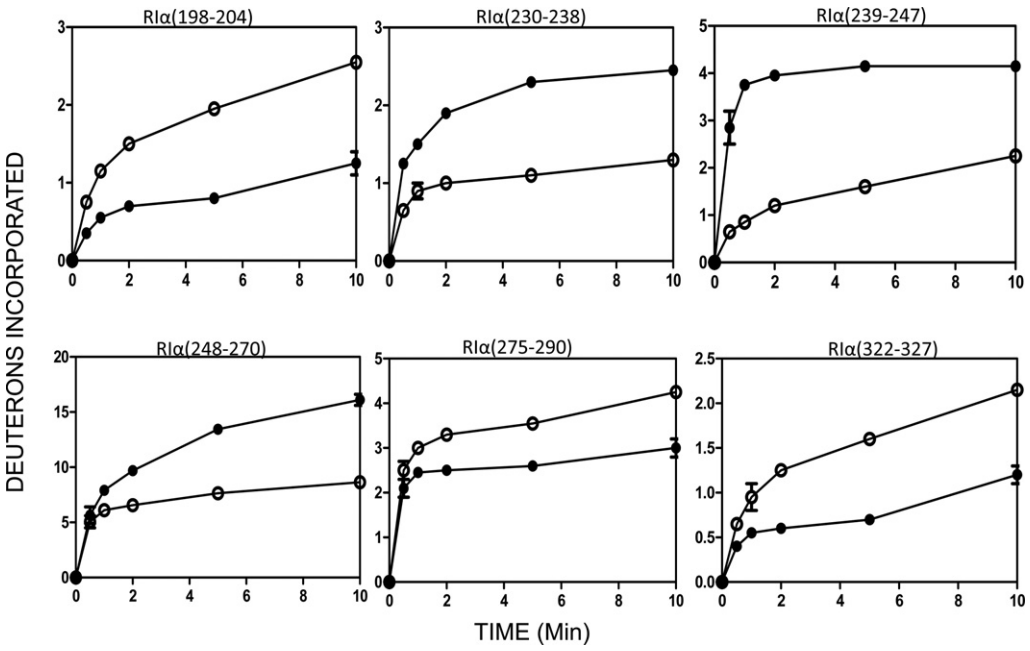

Fig. 4. Time-course (0.5–10 min) of deuterium exchange for peptides from RIα(92–379)R209K. Open circle (○), RIα(92–379)R209K:C in the absence of cAMP; close circle (●), RIα(92–379)R209K:C in the presence of cAMP.

exchange protection seen upon cAMP binding in the free R-subunit was significantly different from that in the cAMP-bound holoenzyme (Figs. 3 and 4 – peptide RIα(322–327)). This presumably reflected the C-subunit-induced long-range conformational changes that affected the dynamics of the CNB-B domain [20,21].

3.4. cAMP binding to CNB-B increases deuterium exchange at interface between CNB-B and C-subunit

Even though the C-subunit does not dissociate upon binding of 1 cAMP molecule to RIα(92–379) R209K:C holoenzyme complex, the R–C interface shows increased deuterium exchange at peptide fragment C (274–296). In the C-subunit, this region corresponds to αH-αI region (site 4 of R–C interface contacts) which contacts the αB:B-αC:B helix (residues 354–362) [4]. Interestingly, the above region from the C-subunit and CNB-B of the R-subunit showed increased exchange (Tables 1 and 2, Fig. 5A) suggesting detachment of CNB-B from the C-subunit. These results reflect cAMP-induced conformational changes within the CNB-B domain leading to partial disruption of the R–C holoenzyme interface.

3.5. Effects of cAMP binding to RIα(92–379)R209K:C holoenzyme: Changes in PBC:A of RIα

Upon binding of cAMP, 1 region in PBC:A spanning residues 198–204 (Figs. 3 and 4 – peptide RIα(198–204)) showed decreased exchange while another region, RIα(202–212) and RIα(202–217) showed increased exchange upon cAMP binding to PBC:B. We believe this indicates that cAMP binding to the CNB-B induces long-range conformational changes within PBC:A and the altered amide exchange is reflective of that.

Comparison of cAMP-bound RIα(92–379)R209K:C holoenzyme and cAMP-bound RIα(92–379)R209K subunit (Table 1, Fig. 5B) showed higher exchange in cAMP-bound RIα(92–379)R209K subunit within the PBC:A also reflecting the long-range allosteric and direct binding effects of C-subunit on the dynamics of CNB-A [20,21].

3.6. Global conformational changes in RIα

In the process of activation of holoenzyme, cAMP binds to CNB-B first followed by CNB-A leading to dissociation of the C-subunit [8]. Addition of cAMP to the RIα (92–379)R209K:C showed extensive changes in amide exchange throughout the molecule, beyond the cAMP binding sites in the two domains. These are summarized below:

3.6.1. Pseudosubstrate region

The N-terminal pseudosubstrate region fragments, (101–106), (111–125) and αA:A region fragment, (136–149) in RIα(92–379)R209K:C holoenzyme showed lower deuterium exchange when compared to the cAMP-bound RIα(92–379)R209K. Barring one segment spanning residues 126–135 obtained from subtractive analysis, that showed increased deuterium exchange in the holoenzyme upon binding of a single molecule of cAMP, all above regions in holoenzyme did not show any difference in deuterium exchange upon cAMP binding to the CNB-B. This reflects overall retention of integrity of the holoenzyme in the absence of a second molecule of cAMP stably binding CNB-A.

3.6.2. αB/C:A, αC′:A and αA:B helix

The αB/C:A and αC′:A helices connect CNB-A and B of R-subunit and undergoes a large conformational change between the C-subunit bound H-form and the cAMP-bound B-form [4]. The fragments, (230–238), (239–247) and (248–254) which cover αB/C:A and αC′:A helices show greatly increased amide exchange in the holoenzyme complex bound to a single molecule of cAMP at CNB-B (Figs. 3 and 4 – peptides, RIα(230–238), RIα(239–247)). We believe that this increased exchange that is seen only in the single cAMP-bound intermediate is reflective of greater conformational mobility [22]. The peptide (248–270) showed significantly greater exchange (Figs. 3 and 4 – peptides RIα(248–270)) upon addition of 1 molecule of cAMP and spans helices αC:A, αC′:A and αA:B (Fig. 5B). Interestingly, αA:B helix forms the bridge that communicates the signal associated with binding of cAMP to CNB-B to CNB-A. The positioning of this helix is greatly shifted in structures of the cAMP-bound and C-subunit-bound states (Fig. 6A and B). Several key residues

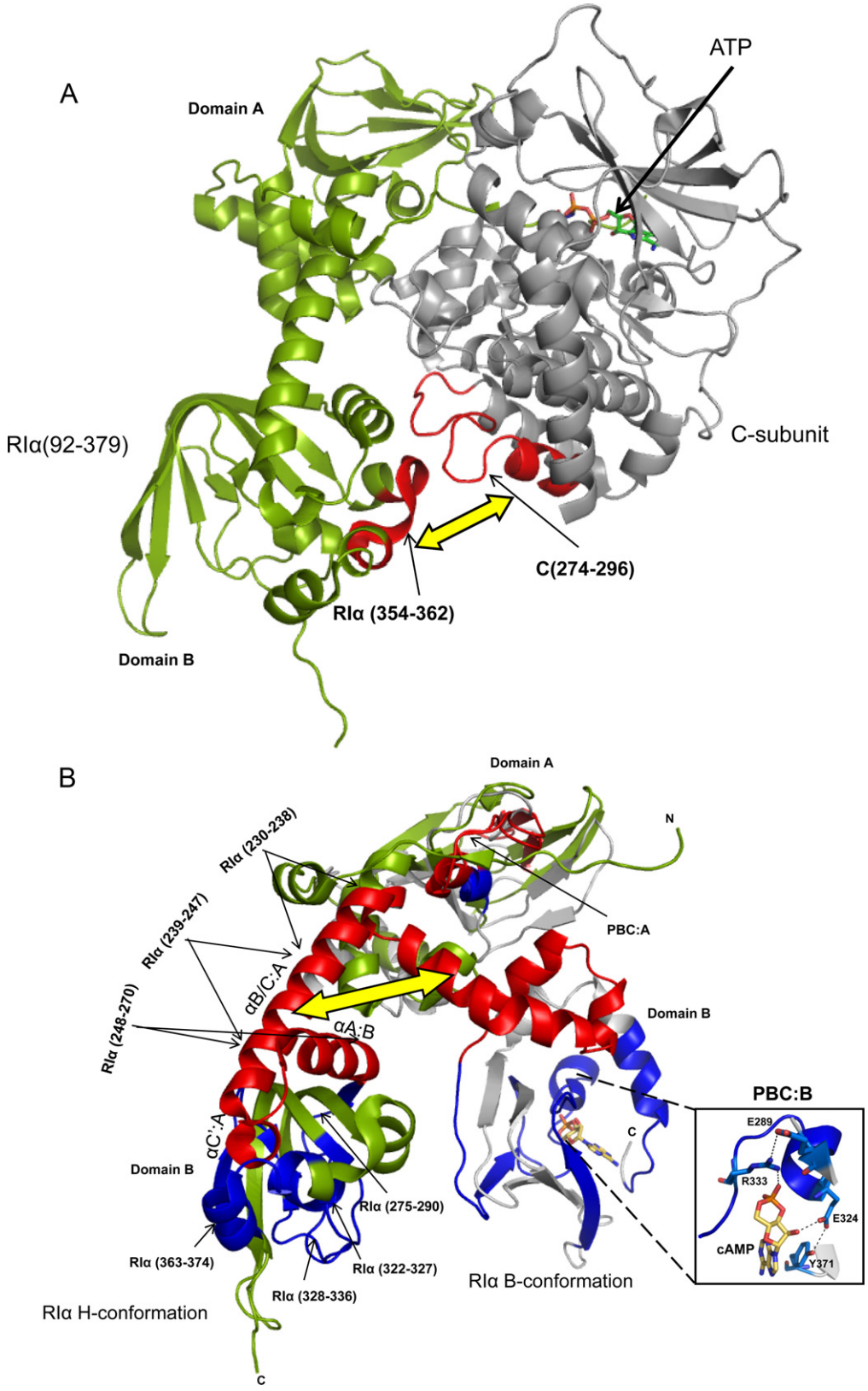

Fig. 5. A: cAMP binding to the CNB-B domain shows increased exchange at the CNB-B:C-subunit interface of the PKA R:C holoenzyme. The R-subunit and the C-subunit are shown in green and gray respectively. Regions showing increased exchange upon binding cAMP are in red and suggest disruption of the specific intersubunit contacts mediated by the CNB-B domain with the C-subunit (yellow arrow), (site 4 of R–C intersubunit interactions [4]). B: Increased exchange upon binding of a single molecule of cAMP to RIα(92–379) R209K:C holoenzyme, within residues 230-270 (spanning αB/C:A and αA of CNB-B) region of the R-subunit reflects increased dynamics and is shown in red. This region reflects the large conformational changes between the H (green) and B (gray)-conformations shown by superposition of PBC:A of cAMP-bound RIα (113–379) (PDB ID: 1RGS) and PBC:A of C-subunit-bound RIα (92–379) (PDB ID: 2QCS). The yellow arrow shows alternate positioning of αB/C:A helix between the H and the B forms. Regions spanning PBC:B show decreased exchange upon binding of cAMP (blue). The inset figure shows residues that are critical for cAMP binding to PBC:B.

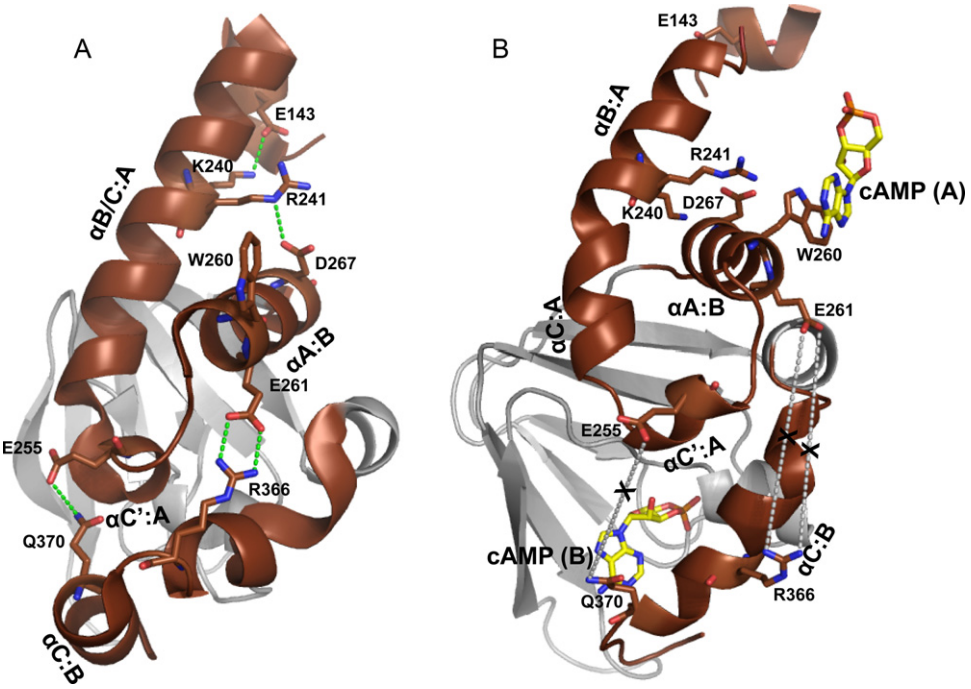

Fig. 6. Importance of CNB-B αA in mediating allosteric cooperativity in the cAMP-activation of PKA. Crystal structure of RIα(92–379) in C-subunit bound, H-conformation (A) (PDB ID: 2QCS) is compared with the crystal structure of RIα(113–379) in cAMP-bound conformation, B-form (B) (PDB ID: 1RGS). Regions showing salt bridges between Q370-E255, E261-R366, R241-D267 and E143-K240 are critical when the R-subunit is in the H-conformation. Binding of a single molecule of cAMP to CNB-B leads to disruption of these critical salt bridges and increases the mobilities of αA:B and α B/C:A helices. The increased mobility positions the critical anchoring residue, W260 to facilitate and stabilize binding of a second molecule of cAMP at CNB-A, leading to activation of PKA.

including Trp 260, a hydrophobic capping residue for cAMP bound to PBC-A, are part of αA:B [1,4]. It is to be noted that 6 amides out of a total of 10 exchangeable amides spanning this helix are completely exchanged with solvent deuterons upon binding of cAMP. Interestingly, the cAMP-bound R-subunit showed lower exchange in this region comparable to C-subunit-bound holoenzyme complex. This suggests that binding of a single cAMP molecule at CNB-B domain shows increased protein mobilities at this region. This contributes to a large difference in conformational entropy as seen in cAMP-bound intermediates in Catabolite Activator Protein (CAP) [22]. In such a model, the end-point B and H-conformations show reduced conformational dynamics compared to the single cAMP-bound intermediate, clearly highlighting the high conformational entropic penalty that accompanies binding of the second molecule of cAMP to CNB-A of wild-type RIα [21]. This clearly explains the negative cooperativity seen in CAP but not the positive cooperativity (Hill coefficient > 1) seen in activation of type I PKA [4,23]. We attribute the positive cooperativity to the increased dynamics in this segment facilitating ordering of the critical aromatic capping residue – Trp 260 which although lies within CNB:B domain, is essential for stable binding of cAMP to CNB:A. It must be noted that the RIα(92–379)(W260A) mutation shows a greatly reduced Hill coefficient (∼0.9 compared to 1.5 for wild-type RIα(92–379):C holoenzyme) [4]. Thus even though the increased dynamics of the intermediate would have predicted an entropic penalty contributing to negative cooperativity, this is offset by the increased sampling of preferred W260-cAMP orientations to facilitate stable capping of cAMP-bound to CNB:A. This effect is likely to be less pronounced in the other CNB-containing proteins including CAP which lack a conserved aromatic capping residue [1]. The increased dynamics in this region reflected by the high amide exchange seen in this segment of the single cAMP-bound intermediate together with the complementary information from X-ray crystallography of the two end-point conformations and extensive biochemistry [1] thus clearly defines the basis for the contribution of the CNB-B domain to cooperativity in the cAMP-dependent activation of PKA. Higher exchange at this region is also consistent with loss of a salt bridge between Glu 261–Arg 366 of RIα-subunit in the H conformation [4].

4. Conclusion

Our study has highlighted a powerful application of amide H/D exchange mass spectrometry in characterizing transient intermediates in the activation cycles of large protein complexes not easily amenable by other structural biology tools such as NMR and X-ray crystallography. Our results on the cAMP-dependent activation of type I PKA clearly demonstrate the important role of the CNB-B domain in mediating the cooperative and allosteric cAMP-dependent activation of PKA. By using a point mutant that abolishes high-affinity binding of cAMP to the CNB-A site, we demonstrate the conformational properties of an intermediate bound to a single molecule of cAMP. Binding of cAMP to CNB-B increases amide exchange at one of the four sites of R–C intersubunit interactions, suggesting that conformational changes associated with cAMP binding at the CNB-B domain partially disrupt intersubunit interactions without leading to dissociation of the C-subunit. Another important result is the increased exchange seen upon cAMP binding at two key regions, the αC/C′:A helix and the αA:B helix. Both these regions are critical in relaying the effects of cAMP binding to CNB-B to CNB-A. The increased exchange in these two regions exclusively in the cAMP-bound to the RIα(92–379)R209K:C holoenzyme but not cAMP-bound to RIα(92–379)R209K specifically highlights the role of CNB-B domain in facilitating the cooperative cAMP-dependent activation of PKA by potentially enhancing affinity of binding of a second molecule of cAMP to CNB-A domain. Our results provide unique insights into the role of CNB-B domain and its communication with CNB-A domain to allow a coordinated and cooperative regulation of PKA where the two domains function as closely coupled rather than individual isolated domains.

Our results highlight the unique capabilities of amide H/D exchange mass spectrometry in structural biology in understanding regulatory cycles of enzyme complexes. It is uniquely poised to probe conformational dynamics of transient reaction intermediates and presents a powerful tool for obtaining mechanistic insights on allostery in enzyme regulation.

Acknowledgements

We thank Mr. Lim Teck Kwang for technical assistance and members of the Anand group for helpful discussions.

References

[1] H.M. Berman, L.F. Ten Eyck, D.S. Goodsell, N.M. Haste, A. Kornev, S.S. Taylor, The cAMP binding domain: an ancient signaling module, Proc. Natl. Acad. Sci. U.S.A. 102 (2005) 45–50.
[2] D.A. Johnson, P. Akamine, E. Radzio-Andzelm, M. Madhusudan, S.S. Taylor, Dynamics of cAMP-dependent protein kinase, Chem. Rev. 101 (2001) 2243–2270.
[3] P.S. Amieux, G.S. McKnight, The essential role of RI alpha in the maintenance of regulated PKA activity, Ann. N. Y. Acad. Sci. 968 (2002) 75–95.
[4] C. Kim, C.Y. Cheng, S.A. Saldanha, S.S. Taylor, PKA-I holoenzyme structure reveals a mechanism for cAMP-dependent activation, Cell 130 (2007) 1032–1043.
[5] Y. Su, W.R. Dostmann, F.W. Herberg, K. Durick, N.H. Xuong, L. Ten Eyck, S.S. Taylor, K.I. Varughese, Regulatory subunit of protein kinase A: structure of deletion mutant with cAMP binding domains, Science 269 (1995) 807–813.
[6] J. Zheng, D.R. Knighton, L.F. ten Eyck, R. Karlsson, N. Xuong, S.S. Taylor, J.M. Sowadski, Crystal structure of the catalytic subunit of cAMP-dependent protein kinase complexed with MgATP and peptide inhibitor, Biochemistry 32 (1993) 2154–2161.
[7] C. Kim, N.H. Xuong, S.S. Taylor, Crystal structure of a complex between the catalytic and regulatory (RIalpha) subunits of PKA, Science 307 (2005) 690–696.
[8] F.W. Herberg, S.S. Taylor, W.R. Dostmann, Active site mutations define the pathway for the cooperative activation of cAMP-dependent protein kinase, Biochemistry 35 (1996) 2934–2942.
[9] D. Ogreid, S.O. Doskeland, Cyclic nucleotides modulate the release of [3H] adenosine cyclic 3′,5′-phosphate bound to the regulatory moiety of protein kinase I by the catalytic subunit of the kinase, Biochemistry 22 (1983) 1686–1696.
[10] E.T. McNicholl, R. Das, S. SilDas, S.S. Taylor, G. Melacini, Communication between tandem cAMP binding domains in the regulatory subunit of protein kinase A-Ialpha as revealed by domain-silencing mutations, J. Biol. Chem. 285 (2010) 15523–15537.
[11] A.N. Hoofnagle, K.A. Resing, N.G. Ahn, Protein analysis by hydrogen exchange mass spectrometry, Annu. Rev. Biophys. Biomol. Struct. 32 (2003) 1–25.
[12] G. Anand, S.S. Taylor, D.A. Johnson, Cyclic-AMP and pseudosubstrate effects on Type-I A-kinase regulatory and catalytic subunit binding kinetics, Biochemistry 46 (2007) 9283–9291.
[13] F.W. Herberg, S.M. Bell, S.S. Taylor, Expression of the catalytic subunit of cAMP-dependent protein kinase in *Escherichia coli*: multiple isozymes reflect different phosphorylation states, Protein Eng. 6 (1993) 771–777.
[14] T.E. Wales, K.E. Fadgen, G.C. Gerhardt, J.R. Engen, High-speed and high-resolution UPLC separation at zero degrees celsius, Anal. Chem. 80 (2008) 6815–6820.
[15] R.H. Bateman, R. Carruthers, J.B. Hoyes, C. Jones, J.I. Langridge, A. Millar, J.P. Vissers, A novel precursor ion discovery method on a hybrid quadrupole orthogonal acceleration time-of-flight (Q-TOF) mass spectrometer for studying protein phosphorylation, J. Am. Soc. Mass Spectrom. 13 (2002) 792–803.
[16] J.C. Silva, R. Denny, C.A. Dorschel, M. Gorenstein, I.J. Kass, G.Z. Li, T. McKenna, M.J. Nold, K. Richardson, P. Young, S. Geromanos, Quantitative proteomic analysis by accurate mass retention time pairs, Anal. Chem. 77 (2005) 2187–2200.
[17] S.J. Geromanos, J.P. Vissers, J.C. Silva, C.A. Dorschel, G.Z. Li, M.V. Gorenstein, R.H. Bateman, J.I. Langridge, The detection, correlation, and comparison of peptide precursor and product ions from data independent LC–MS with data dependant LC–MS/MS, Proteomics 9 (2009) 1683–1695.
[18] G.Z. Li, J.P. Vissers, J.C. Silva, D. Golick, M.V. Gorenstein, S.J. Geromanos, Database searching and accounting of multiplexed precursor and product ion spectra from the data independent analysis of simple and complex peptide mixtures, Proteomics 9 (2009) 1696–1719.
[19] D.D. Weis, J.R. Engen, I.J. Kass, Semi-automated data processing of hydrogen exchange mass spectra using HX-Express, J. Am. Soc. Mass Spectrom. 17 (2006) 1700–1703.
[20] G.S. Anand, C.A. Hughes, J.M. Jones, S.S. Taylor, E.A. Komives, Amide H/2H exchange reveals communication between the cAMP and catalytic subunit-binding sites in the R(I)alpha subunit of protein kinase A, J. Mol. Biol. 323 (2002) 377–386.
[21] Y. Hamuro, G.S. Anand, J.S. Kim, C. Juliano, D.D. Stranz, S.S. Taylor, V.L. Woods Jr., Mapping intersubunit interactions of the regulatory subunit (RIalpha) in the type I holoenzyme of protein kinase A by amide hydrogen/deuterium exchange mass spectrometry (DXMS), J. Mol. Biol. 340 (2004) 1185–1196.
[22] N. Popovych, S. Sun, R.H. Ebright, C.G. Kalodimos, Dynamically driven protein allostery, Nat. Struct. Mol. Biol. 13 (2006) 831–838.
[23] F.W. Herberg, W.R. Dostmann, M. Zorn, S.J. Davis, S.S. Taylor, Crosstalk between domains in the regulatory subunit of cAMP-dependent protein kinase: influence of amino terminus on cAMP binding and holoenzyme formation, Biochemistry 33 (1994) 7485–7494.
[24] G.S. Anand, S. Krishnamurthy, T. Bishnoi, A. Kornev, S.S. Taylor, D.A. Johnson, Cyclic AMP- and (Rp)-cAMPS-induced conformational changes in a complex of the catalytic and regulatory (RIalpha) subunits of cyclic AMP-dependent protein kinase, Mol. Cell Prot. 9 (2010) 2225–2237.